RevMexAA (Serie de Conferencias), **14**, 85–89 (2002)

SCALING RELATIONS OF SPIRAL GALAXIES AND THEIR APPLICATION TO COSMOLOGY

R. Giovanelli[1]

Department of Astronomy, Space Sci. Bldg., Cornell University, NY 14853, USA

RESUMEN

La justificación teórica de las principales relaciones de escala para las galaxias espirales se discute brevemente, y se nota que la mejor determinada entre ellas es la que se obtiene entre luminosidad y velocidad rotacional (TFR). Además se discuten las fuentes de dispersión para dichas relaciones de escala. Se resumen los resultados de aplicaciones de la TFR a la Cosmología, en particular los estimados de $H_\circ$, de la linearidad del flujo de Hubble, del campo de velocidades peculiares y su convergencia, y del parámetro de densidad de masa.

ABSTRACT

The theoretical background for the main scaling relations of spiral galaxies is discussed, and compared with the observational datum. The luminosity–linewidth relation (TFR) is the best determined among those; the sources of scatter of each are discussed. The results of applications of the TFR to Cosmology, using several all–sky samples of galaxies, are summarized. They yield estimates of $H_\circ$, of the linearity of the Hubble flow, of the peculiar velocity field and its convergence depth and of the mass density parameter.

Key Words: **GALAXIES: SPIRAL — COSMOLOGY: OBSERVATIONAL**

1. SCALING RELATIONS: BACKGROUND

In the most successful theoretical framework for the rise of structure in the Universe, small fluctuations in the mass distribution are driven by gravitational instability, merge and grow hierarchically. Within it, and as indicated by a growing body of observational evidence, the baryonic matter fraction of the cosmic energy density is largely exceeded by the non–baryonic component, composed of non–relativis– tic, collisionless particles; hence the reference to a cold dark matter (CDM) scenario. An even larger fraction of the cosmic energy density may be contributed by some form of dark energy, a component of still undetermined equation of state. This cold dark matter (CDM) scenario, and its adaptation to a model including dark energy (ΛCDM), have been relatively succesful in explaining many of the observational properties of the galaxy clustering, evolution and structure.

In the description of disks and their evolution, a useful metric is the dimensionless spin parameter λ, which represents the degree to which a system is rotationally supported against collapse. An elliptical galaxy has $\lambda \simeq 0.05$, while the spin parameter of a spiral disk is $\simeq 0.5$. CDM N–body simulations show that, when halos decouple from the Hubble flow, the build–up of angular momentum via tidal torques ceases, yielding a distribution of λ parameters with a median value near 0.05, and with only 10% of halos having λ larger than 0.1 or smaller than 0.025. From this state, later evolution causes spiral disks to become rotationally supported with $\lambda_{disk} \sim 0.5$, via dissipative collapse of the baryons. As disks settle in exponential configurations, and if halos are approximated by isothermal spheres, this disk formation paradigm leads naturally to a set of scaling relations between disk mass M_d, scalelength R_d, central mass surface density $\Sigma_\circ$ and rotational speed V_{circ}, namely (Mo et al. 1998):

$$R_d \propto \lambda (j_d/m_d)[H(z)/H_\circ]^{-1} V_{circ} \quad (1)$$

$$\Sigma_\circ \propto \lambda^{-2} m_d (j_d/m_d)^{-2} [H(z)/H_\circ] V_{circ} \quad (2)$$

$$M_d \propto m_d [H(z)/H_\circ]^{-1} V_{circ}^3 \quad (3)$$

where m_d is the mass fraction of the disk, j_d its angular momentum fraction, λ the spin parameter *of*

[1]Email: riccardo@astro.cornell.edu

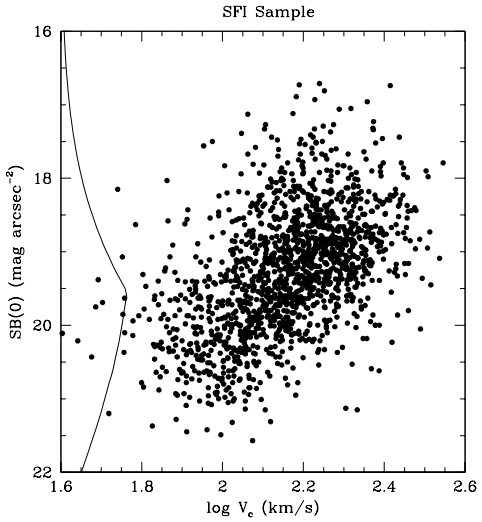

Fig. 1. Scalength vs. rotational velocity for the SFI sample. Data are the same in both panels. Curves represent expectations from Eqn. (1) for a standard CDM (upper panel) and a ΛCDM ($\Omega_\Lambda = 0.65$; lower panel) cosmology. In each case, expected relations are computed for three different formation redshifts (solid lines for $z_f = 0$, short dashes for $z_f = 0.5$ and long dashes for $z_f = 1$, while for each of those cases, the relation for halo $\lambda = 0.025, 0.05, 0.1$ is shown.

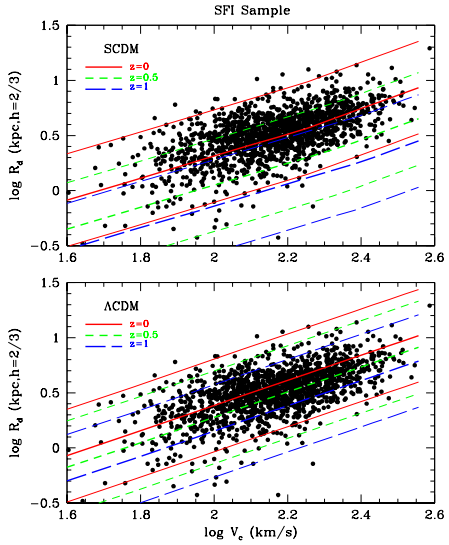

Fig. 2. Relation between central disk surface brightness at I band and rotational velocity. The solid line on the left describes the selection function of the sample.

the halo, $H(z)$ the value of the Hubble parameter at the redshift of assembly of the disk and $H_\circ$ its present value. That halos are singular isothermal spheres is a simplistic assumption. If more elaborate halo profiles are adopted (e.g. that of Navarro, Frenk & White 1997, as suggested by CDM N–body simulations), Eqns. (1–3) can be modified by simply multiplying them by dimensionless factors of order of unity, which take into consideration variance in the degree of concentration of halos, the shape of the rotation curves and the radius at which V_{circ} is to be measured.

Introducing a disk mass–to–light ratio $\Upsilon_d \equiv M_d / L_d$, Eq. (3) can be recognized as the Tully–Fisher relation (TFR) $L_d = A\, V_{circ}^{\alpha}$. The explicit power law dependence of L_d on V_{rot} in Eq. (3), with $\alpha = 3$, is close to that obtained from observations, although full agreement between theory and observation could only be claimed if theory could justify that the product $A \propto m_d \Upsilon_d^{-1} [H(z)/H_\circ]^{-1}$ is independent of V_{circ}, an uneasy assumption. Eqns. (1–3) suggest that the sources of scatter in disk scaling relations are to be found in the variances of m_d, j_d, Υ_d and halo λ. Numerical simulations and heuristic arguments provide some aid in estimating those variances, those on Υ_d requiring simulations that incorporate hydrodynamical and spectral energy distribution evolution calculations, some of which are computationally challenging (e.g. Navarro & Steinmetz 2000 and refs. therein) While the CDM paradigm proposes an overall picture of increasing coherence, problems with it do however remain, as underscored in a number of studies. Sellwood & Kosowsky (2000) provide a list of the main criticisms to the CDM scenario, as they apply specifically in the context of the structure of galaxies.

2. SCALING RELATIONS: OBSERVATIONS

In this section, we confront Eqns. (1–3) with observational data from three all-sky galaxy samples of ours, each including I band CCD photometry and rotational widths for late spiral galaxies. In Figure 1, the scaling relation represented by Eqn. (1) is shown for field galaxies within $cz \sim 7500$ km s^{-1} (SFI). The slope predicted by Eqn. (1) is reproduced, and the data are consistent with relatively late disk formation epochs. Figure 2 shows the relationship between central disk surface brightness and rotational width for the SFI sample; for a constant mass–to–light ratio, Eqn. (2) predicts a

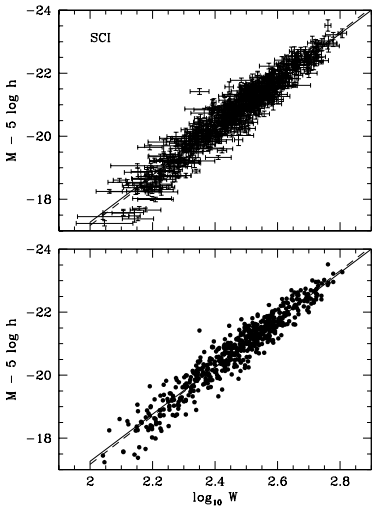

Fig. 3. TFR for the SCI sample of 780 galaxies in 24 nearby clusters. The upper panel shows measurement errors, the lower panel shows data points without error bars. The width W is twice the rotational velocity V_c.

slope of 5, not too dissimilar from that observed in Figure 2. Estimates of scalelengths and central disk surface brightness are notoriously dicey, and some of the scatter observed is due to that uncertainty. In addition, particularly in Figure 2, observational biases affect the observed distribution of the data, suggesting caution in interpreting the results. Figure 3 displays the tightest among the spiral galaxy scaling relations, as obtained for a sample of cluster spirals within $cz \sim 9000$ km s^{-1} (SCI); the slope is very close to the explicit dependence on V_c^3 in Eqn. (3), implying that the product $m_d \Upsilon_d^{-1} [H(z)/H_\circ]^{-1}$ is indeed nearly independent of V_c, in spite of the fact that m_d and Υ_d are known to independently vary with V_c.

The "zero points" of relations (3), (1) and (2) are expected to depend respectively on λ^0, λ^1 and λ^2. As N–body simulations show that the scatter in halo λ values to be roughly $\delta\lambda/\bar{\lambda} \simeq 0.5$, this variance should add scatter of amplitude ± 0.3 in $\log R_d$ and ± 1.5 mag in $SB(0)$, thus suggesting that much of the observed scatter in Figs. 1–2 arises from variance in halo λ values.

It should be pointed out that attempts at obtaining a relation tighter than TFR (i.e. a better representation of a fundamental plane for spirals) have

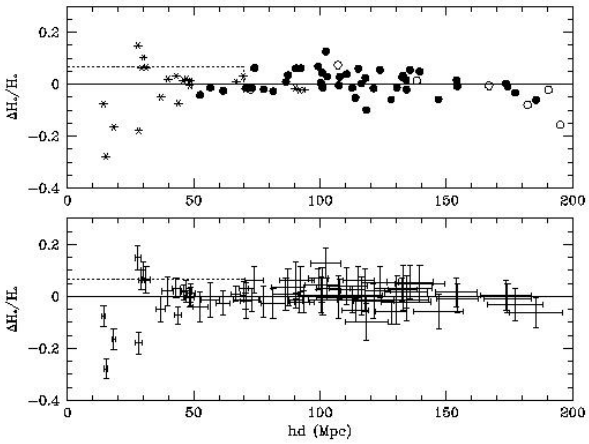

Fig. 4. Fluctuations in the Hubble flow, as measured for 75 clusters of galaxies via TFR. Lower panel displays error bars on data points shown in upper panel. At small distances, the peculiar velocities of individual clusters are significant, in comparison with their Hubble velocity, producing the large scatter observed.

proven ineffective. The TFR appears to be pretty close to an edge–on view of such fundamental plane.

3. COSMOLOGICAL APPLICATIONS

Hubble Constant and Linearity of the Hubble Flow.
Given an accurate TFR template, and a set of redshift–independent distances (e.g. via Cepheids) for a small set of objects, a fair estimate of $H_\circ$ can be obtained, which will be *independent* on the peculiar velocity of the distance calibrators. Using this approach, we have determined $H_\circ = 69 \pm 7$ km s^{-1} Mpc^{-1} , on the basis of a dozen Cepheid calibrators (Giovanelli et al. 1997 (ApJ, 477, L1)), a result confirmed by the independent determination of Sakai et al. (2000). TFR can also be used effectively in gauging the linearity of the Hubble flow. Recently, Zehavi et al. (1998) suggested that the large values of $H_\circ$ estimated by some from local objects may be due to the Local Group (LG) being near the center of an underdense bubble with a radius of some 7000 km s^{-1} ; this would produce a change in $H_\circ$ near that cz. We have used a set of 75 clusters (Giovanelli et al. 1999 (ApJ, 525, 25)) with peculiar velocities measured via TFR, to gauge variations in the Hubble flow $\Delta H_\circ/H_\circ$, to $cz = 20,000$ km s^{-1} , and find no evidence of any systematic acceleration of the Hubble flow within that volume (see Fig. 4).

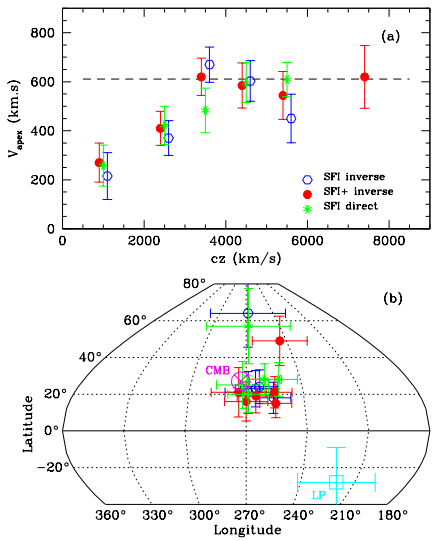

Fig. 5. Amplitude (upper panel) and direction in galactic coordinates (lower panel) of the reflex motion of the LG with respect to SFI galaxies pertaining to different redshift shells. Different symbols in the upper panel correspond to determinations of V_{pec} using different techniques. The large square in the lower panel is the LP94 dipole, while the large circle with a cross is the CMB dipole direction.

Convergence Depth.
The CMB dipole provides us with an accurate measure of the LG's peculiar velocity (V_{pec}), which has an amplitude of $V_{dip} = 620$ km s^{-1} in the reference frame where the CMB dipole is null. This motion is caused by mass density fluctuations $\delta_m(\mathbf{r})$ in the local Universe; those within a spherical shell of radius R produce a contribution to the LG's V_{pec}

$$\mathbf{V}_{pec,LG}(R) = \frac{H_\circ \Omega_m^{0.6}}{4\pi} \int \delta_m(\mathbf{r}) \frac{\mathbf{r}}{r^3} W(r,R) d^3\mathbf{r} \quad (4)$$

where $W(r,R)$ is a window function of width R and Ω_m the cosmological matter density. Asymptotically, $V_{pec,LG}(R \to \infty) = V_{dip}$. How large need R be for convergence between $V_{pec,LG}(R)$ and V_{dip}? This is one of the fundamental questions of Cosmology. In Fig. 5, the reflex motion of the LG with respect to the SFI galaxies, subdivided in shells of increasing radius, is shown. It is clear how convergence, as defined above, appears to be achieved — *both in amplitude and direction* — at radii near 4–5000 km s^{-1} (Giovanelli et al. 1998 (ApJ, 505, L91)). The SFI sample does however not extend much farther than that convergence depth. It is thus conceivable that the observed convergence is not maintained at larger distances, especially in consideration of results from other groups (Lauer & Postman 1994, SMAC's Smith et al. 2000), which claim large bulk flows over scales larger than 10^4 km s^{-1} . Dale et al. (1999) have thus sought to verify whether convergence still holds at a distance twice that mapped by the SFI sample. Our sample SC2 includes more than 500 galaxies in 50 clusters at a median $cz \simeq 12,000$ km s^{-1} . Fig. 6 shows the dipole of that cluster sample, which covers the whole sky, plotted in stereographic form in Cartesian supergalactic coordinates. SC2 shows that convergence is still valid for this sample, indicating that no large–scale bulk flow is present over scales in excess of ~ 5000 km s^{-1} .

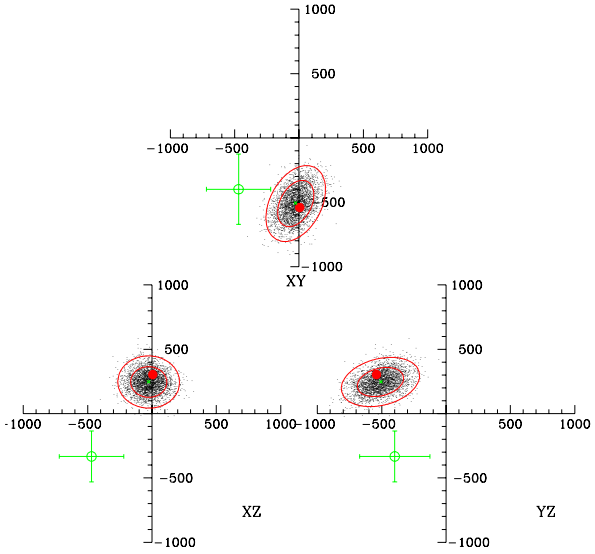

Fig. 6. Dipole of the SC2 sample of Dale et al.(1999). The large cross is th eLP94 dipole; the large solid circle is the CMB dipole. The clouds of data points illustrate the probability density of the SC2 dipole.

Estimates of Ω_m. The peculiar velocity field provides the tool for the determination of the cosmological mass density, which can be obtained via several different techniques. The V_{pec} field is nearly insensitive to Ω_Λ. In various collaborations (see Branchini et al. 2001 and references therein), SFI and SCI have been used to determine Ω_m, generally yielding values between 0.25 and 0.5.

REFERENCES

Branchini, E. et al. 2001, MNRAS, 326,1191
Dale, D. et al. 1999, ApJ, 510, L11
Lauer, T. & Postman, M. 1994, ApJ, 425, 418
Mo, H., Mao, S. & White, S. 1998, MNRAS, 295, 319
Navarro, J., Frenk, C. & White, S. 1997, ApJ, 487, 73
Navarro, J. & Steinmetz, M. 2000, ApJ, 538, 477
Sakai, S. et al. 2000, ApJ, 529, 698
Sellwood, J. & Kosowsky, A. 2000, astro–ph/0009074
Smith, R. et al. 2000, PASP Conf. Series, vol 201, p. 39
Zehavi, I. et al. 1998, ApJ, 503, 483